16th World Conference on Earthquake, 16WCEE 2017

Santiago Chile, January 9th to 13th 2017

Paper N° 2543 (Abstract ID)

Registration Code: S- X1462787108

A discrete simulation tool for the study of old masonry nonlinear behavior

C. Giry[(1)], C. Limoge[(2)], M. Vassaux[(3)], F. Ragueneau[(4)]

[(1)] *Associate Professor, LMT-Cachan, ENS Cachan, CNRS, Université Paris Saclay, 61, avenue du Président Wilson, 94235 Cachan, France, cedric.giry@ens-cachan.fr*

[(2)] *Dr., LMT-Cachan, ENS Cachan, CNRS, Université Paris Saclay, 61, avenue du Président Wilson, 94235 Cachan, France, limoge@lmt.ens-cachan.fr,*

[(3)] *Dr., LMT-Cachan, ENS Cachan, CNRS, Université Paris Saclay, 61, avenue du Président Wilson, 94235 Cachan, France, vassaux@lmt.ens-cachan.fr*

[(4)] *Full Professor, LMT-Cachan, ENS Cachan, CNRS, Université Paris Saclay, 61, avenue du Président Wilson, 94235 Cachan, France, ragueneau@lmt.ens-cachan.fr*

Abstract

Seismic assessment of historical masonry structures is a crucial field of architectural heritage. However, for this kind of structures, it may be difficult to get information relative to the mechanical properties of the masonry itself. Indeed, as the structures may generally be protected as cultural heritage, no sample of the material can be extracted in order to characterize it. As a consequence, it may be difficult to assess the vulnerability of this type of structures face to seismic loadings. In this paper, a strategy is proposed in order to tackle this problem. In recent works, a discrete simulation tool has been developed to analyze and characterize the behavior of concrete. This tool, based on discrete elements method, allows investigating the response of quasi-brittle materials submitted to different loadings like uniaxial cyclic loading, shear loading, ... The media is described with rigid particles with beam elements between them reproducing the cohesion of the material. Contact laws are also introduced in the model in order to describe the behavior during crack closure. This work proposed an adaptation of this virtual testing tool for old masonry. Through a case study dealing with baroque religious heritage in French Savoy, a continuous damage model which parameters are identified from numerical experiments is used in order to analyze the response of a church under seismic loading. An analysis of the nonlinearities observed in the simulation is proposed with a comparison with "classical" failure mechanism of masonry churches under seismic loading.

Keywords: old masonry; discrete element method; virtual testing; damage model.

1. Introduction

Recent events have shown that the preservation of masonry Cultural Heritage Structure (CuHeS) against seismic hazard is of main concern and needs preventive assessments. In this context, it is necessary to propose efficient tools capable of taking into account all the possible ruin mechanisms of the studied structure. However, this problem still represent a challenge as old masonry displays complex mechanical behaviors. In fact, it is characterized by its composite nature, formed by discrete units of stones or bricks, separated by dry or mortared joints, and possibly infilling materials. Its tensile strength is almost null, providing a brittle tensile response, explained by the low tensile strength of its materials and of the connection between its components. Its shear response is frictional due to cracking and separation along joints once the limited bond between units and mortar is lost. It is also an anisotropic material whose response highly depends on the load orientation. These complex failure modes will be magnified when the structure is subjected to complex loads, such as earthquake.

Old masonry is most often very heterogeneous and irregular, even in a single structure, because it has often been repaired along the structure's life, with various materials. These components can hardly be characterized in order to respect the integrity of the protected CuHes. Protection rules limit the possible tests, pits and cores, on the structure. Therefore, the available information that can be collected is very limited. In this context, virtual testing strategy has to be considered to investigate the complex behavior of old masonry material.

Recent works of some of the authors have proposed a virtual testing tool to identify the response of quasi-brittle material as concrete under cyclic loadings. This tool, based on discrete element method, provides a framework allowing to represent explicitly the multiple and anisotropic crack openings and their closure as well as the friction between solids. By considering some adjustments of this tool and based on similar works as the one of **Erreur ! Nous n'avons pas trouvé la source du renvoi.**, this approach can be derived for the assessment of the behavior of old masonry.

In order to describe efficiently and rapidly the response of old masonry at structural scale without making too much hypothesis and loosing too much information, a nonlinear continuous homogenized model seems to be still the better choice. However, this kind of model can introduce several parameters that need to be identified. Due to the fact that a few data are available and that some experimental tests can be tricky to manage, the virtual testing tool represents a good candidate to do this task. Combining general data on the real masonry (i.e. compressive strength) and this virtual testing tool, one can get an overall view of the behavior of the material.

In a first part, the beam-particle modeling technique is presented and its capacity to reproduce the behavior of old masonry is investigated. Then, this model is used as a virtual testing tool to identify the parameters of a simple continuous model for which the main equations are described. At the end, a structural application of the identified continuous model is performed, considering the response of a French baroque church under an Alpine recent earthquake.

2. Mesoscopic simulations of old masonry

2.1 Modeling technique

In order to provide a representative response of samples at the material scale, virtual testing needs the introduction of a microscopic model. The framework considered in this work is a 2D particle-based model made of a combination of a Euler-Bernoulli beams network, which is used to reproduce cohesion and the fracture mechanisms between the particles, and of the DEM, which allows realistic crack's interactions description thanks to the integration of contact and friction mechanisms. Unlike classical DEM or Contact Dynamics models, the microscopic model is developed within a quasi-static framework to enable reasonable computational costs and to avoid the introduction of arbitrary dynamic effects. The integration algorithm is an incremental version of classic event driven integration schemes, to allow the computation of the solution as a succession of stable equilibrium states, while accounting for other nonlinearities than fracture, namely contact and friction, which cannot be solved in an event driven fashion.

The equations governing the lattice elastic behavior are summarized in (eq. 1). Two parameters are introduced α, $\bar{E}$, respectively the coefficient of inertia and the Young modulus of the lattice's beams.

$$\boldsymbol{F}_{coh,ij} = \begin{cases} F_{N,ij} = \dfrac{\bar{E} A_{b,ij}}{\ell_{b,ij}} (\boldsymbol{u}_i - \boldsymbol{u}_j).\boldsymbol{n}_{b,ij} \\ F_{T,ij} = \dfrac{12 \bar{E} I_{b,ij}}{{\ell_{b,ij}}^3} (\boldsymbol{u}_i - \boldsymbol{u}_j).\boldsymbol{t}_{b,ij} - \dfrac{6 \bar{E} I_{b,ij}}{{\ell_{b,ij}}^2} (\theta_i - \theta_j) \\ M_{Z,ij} = \dfrac{6\, \bar{E} I_{b,ij}}{{\ell_{b,ij}}^2} (\boldsymbol{u}_j - \boldsymbol{u}_i).\boldsymbol{t}_{b,ij} + \dfrac{4 \bar{E} I_{b,ij}}{\ell_{b,ij}} \left(\theta_i - \dfrac{\theta_j}{2}\right) \end{cases} \quad (1)$$

where $F_{N,ij}$, $F_{T,ij}$ and $M_{Z,ij}$ stand for, respectively, the normal force, the tangent force and the bending moment in the beam linking particles i and j; $\boldsymbol{u}_i$ and θ_i, respectively, the displacements and the rotation of the particle i; $\boldsymbol{n}_{b,ij}$ and $\boldsymbol{t}_{b,ij}$, respectively, for the normal and tangent vectors to the cross-section of the beam linking particles i and j; and $A_{b,ij}$, $I_{b,ij}$ and $\ell_{b,ij}$, respectively, the cross-section, the moment of inertia, and the length.

Failure of lattice's beams is determined using a criterion expressed in function of the beam's strain and the rotation of its ends.

$$\frac{\epsilon_{ij}}{\epsilon_{ij}^{cr}} + \frac{|\theta_i - \theta_j|}{\theta_{ij}^{cr}} > 1 \quad (2)$$

The original particle-based model considered for this work is originally developed for quasi-brittle material such as concrete. For this kind of material, phases are generally not distinctly described, thus statistically distributed failure properties are considered. When employed to model masonry, a simplification can be made, partly due to the discrete mesostructure of masonry (distinction between stones and mortar). As experimentally crack patterns rarely show cracks propagating through stones, one can assume that each discrete polygonal particle (i.e. rigid particle) obtained using a random Voronoi diagram of the masonry structure represents a distinct stone (see Fig. 1).

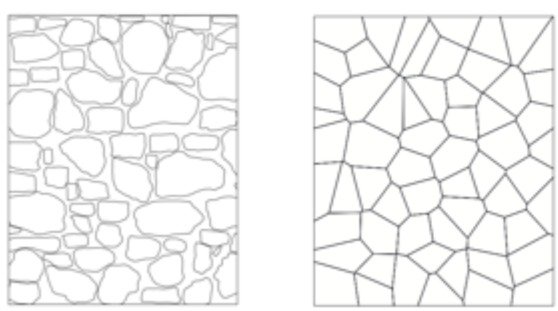

Fig. 1 – Masonry wall: experimental sample (left) and its associated virtual sample (right).

In order to manage the interaction between two distinct parts of the masonry (e.g. two blocks separated by a crack), additional conditions have to be introduced in the code. So when two neighboring particles overlap, if not linked by a cohesive beam, contact forces are generated. The contact force is proportional to the overlap area and to Young modulus of the material, identical to beam's one $\bar{E}$.

$$\boldsymbol{F}_{cont,ij} = \frac{\bar{E} S_{r,ij}}{\ell_{c,ij}} . \boldsymbol{n}_{c,ij} \quad (3)$$

Where $\boldsymbol{F}_{cont,ij}$ stands for the normal contact between the particles i and j in contact, $\boldsymbol{n}_{c,ij}$ stands for normal contact direction, $S_{r,ij}$ stands for the overlap area, and $\ell_{c,ij}$ is a characteristic length supposed to be an average of the diameter of the particles:

$$\ell_{c,ij} = \frac{1}{2}\left(\frac{1}{D_i} + \frac{1}{D_j}\right) \quad (4)$$

In addition, a friction force can be generated in between two contacting particles, following Coulomb friction model, introducing the friction coefficient μ of the stone.

$$\|\boldsymbol{F}_{fric,ij}\| = \min\left(\|\boldsymbol{F}_{fric,ij}^{el}\|, \mu\|\boldsymbol{F}_{cont,ij}\|\right) \quad (5)$$

where $\boldsymbol{F}_{cont,ij}$ and $\boldsymbol{F}_{fric,ij}$ stand respectively for the normal and the tangent frictional forces between two particles i and j in contact. This microscopic model as well as its integration algorithm are thoroughly described in **Erreur ! Nous n'avons pas trouvé la source du renvoi.**. The validation of the model under multi-axial and cyclic loading, and therefore with respect to mixed-mode fracture and contact mechanisms, has been presented in **Erreur ! Nous n'avons pas trouvé la source du renvoi.**.

2.2 Calibration

The model features only six parameters to be calibrated: the particle's size, the lattice Young modulus and coefficient of inertia, the extension and rotation failure thresholds, and the friction coefficient. The adaptation of the model for old masonry leads to the calibration of these parameters with only a single compression test, while in its original application to quasi-brittle materials, several non-elastic tests were required **Erreur ! Nous n'avons pas trouvé la source du renvoi.**.

2.3 Validation for three-leaf stone masonry

Tests conducted by **Erreur ! Nous n'avons pas trouvé la source du renvoi.** on three-leaf stone masonry wall of 1.20 m height, 1.00 m width and 0.50 m thickness are used as reference in order to validate the present model's ability to reproduce masonry behavior. Information provided by a monotonic compression test are used to calibrate the elastic and failure parameters. Validation is completed checking the efficiency of the model to reproduce masonry's shear behavior. Both tests details of the setup can be found in **Erreur ! Nous n'avons pas trouvé la source du renvoi.**.

In practice, the particles dimension is chosen to obtain the same number of stones in the masonry wall. The present reference wall has ten stories of six stones in the wall's surface. Since the mesoscopic model is only 2D, simulated results correspond to a one-meter thick wall. These results are linearly converted to be compared with the experimental results of the half-meter thick wall.

Mesoscopic model's parameters value are resumed in the table 1, as well as the experimental properties provided in **Erreur ! Nous n'avons pas trouvé la source du renvoi.** and used to calibrate the model's parameters (respectively the longitudinal Poisson ratio, the initial Young modulus, the first-crack appearance stress and the peak-load stress).

Table 1 – Experimental data (exp.) and model parameters of the virtual testing (DEM).

Parameters (exp.)	Values	Parameters (DEM)	Values
ν_L (-)	0.19	α	0.80

E (GPa)	2.885	E (GPa)	2.5
$\sigma^{1,cr}$ (MPa)	0.4	ϵ^{cr}	10^{-4}
σ^{max} (MPa)	2.1	θ^{cr}	7.10^{-4}

As the last parameter of the virtual testing (i.e. the friction coefficient μ) can not be identified from the experiments in 0, its value is taken from the literature. Stones friction coefficient is classically assessed to 0.6.

A first verification of the model efficiency lies in checking the monotonic compression response. Although, part of this response has been used to calibrate the model, the global response accuracy is not ensured. The simulated and experimental responses are compared in Fig. 2. The model is able to reproduce qualitatively and quantitatively the overall response up to the peak-load, before a complete brittle failure of the wall occurs.

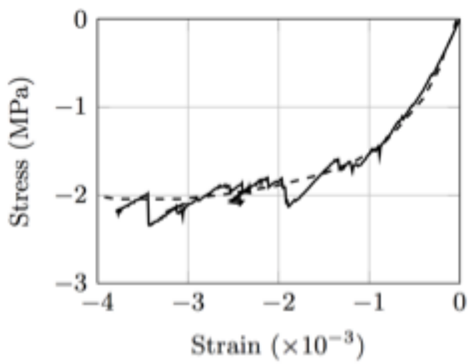

Fig. 2 – Response of the masonry wall under compressive loading (Exp. vs virtual testing).

Validation is then pursued with a shear test under a constant 1 MPa axial compression stress. The simulated and experimental responses are compared in Fig. 3. Masonry used for this test is supposed to be identical to the masonry used for the compression test, therefore model's parameters are left unmodified. The simulated response is quantitatively similar to the experimental response up to an applied displacement of 4 mm. Beyond this applied displacement, experimental and simulated responses slightly part ways, brittle failure is observed at 5 mm numerically, while it is observed at 6 mm experimentally.

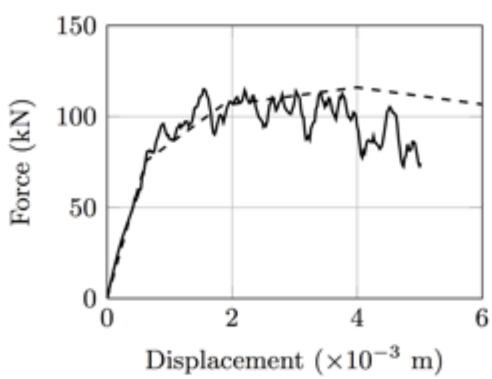

Fig. 3 – Response of the masonry wall under shear loading (Exp. vs virtual testing).

As an additional confirmation of the mesoscopic model's efficiency, the crack pattern at the peak-load (Fig. 4) are quite realistic. No comparison can be made with results provided in **Erreur ! Nous n'avons pas trouvé la**

source du renvoi., nevertheless orientation of cracks is relevant to a shear test, implying that correct failure mechanisms are involved in addition to the correct strength estimations shown in the test's response (Fig. 3).

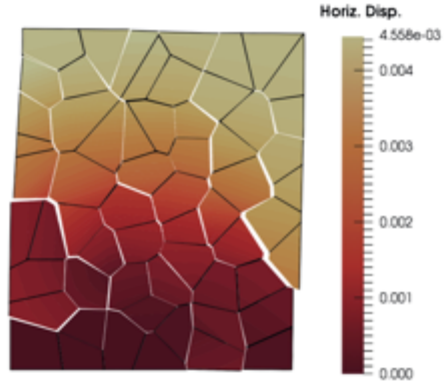

Fig. 4 – Simulated crack pattern under shear loading with 1 MPa compression.

3. Continuous model for structural analysis

3.1 Isotropic continuous damage model

In order to illustrate the methodology and the use of the virtual testing tool presented previously, we consider parameters identification of a simple isotropic damage model. The main equations of this model used to describe the old masonry are recalled. Its formulation can be seen as a simplified version of the one proposed by **Erreur ! Nous n'avons pas trouvé la source du renvoi.**. Despite its simplicity, this model reproduces the dissymmetrical behavior in tension and compression as well as the unilateral effect for cyclic loading. Furthermore, the damage variable is driven by strain quantity providing so an explicit formulation. Its parameters are fitted in this study in accordance with results from the previously exposed numerical experiments for masonry walls.

The damage occurring in the masonry is decomposed in two process: one for tension d^t and one for compression d^c. So, the Helmholtz free energy of the model is expressed as:

$$\rho\psi = (1 - d^t)\psi_0^t + (1 - d^c)\psi_0^c \qquad (6)$$

With $\psi_0^t = \mathcal{H}[\mathrm{Tr}(\widetilde{\boldsymbol{\sigma}})]\boldsymbol{\varepsilon}: \boldsymbol{C}_0: \boldsymbol{\varepsilon}$ and $\psi_0^c = \mathcal{H}\left[\mathrm{Tr}(\text{-}\widetilde{\boldsymbol{\sigma}})\right]\boldsymbol{\varepsilon}: \boldsymbol{C}_0: \boldsymbol{\varepsilon}$. $\boldsymbol{C}_0$ is the fourth-order isotropic linear-elastic constitutive matrix and $\widetilde{\boldsymbol{\sigma}}$ is the effective stress (i.e. $\widetilde{\boldsymbol{\sigma}} = \boldsymbol{\varepsilon}: \boldsymbol{C}_0: \boldsymbol{\varepsilon}$). $\mathcal{H}[.]$ is the Heaviside function.

By deriving Eq.7 according to the strain tensor $\boldsymbol{\varepsilon}$, one can get the expression of the state law:

$$\boldsymbol{\sigma} = (1 - d^t)\mathcal{H}[\mathrm{Tr}(\widetilde{\boldsymbol{\sigma}})]\boldsymbol{C}_0: \boldsymbol{\varepsilon} + (1 - d^c)\mathcal{H}[\mathrm{Tr}(-\widetilde{\boldsymbol{\sigma}})]\boldsymbol{C}_0: \boldsymbol{\varepsilon} \qquad (7)$$

In order to verify the thermodynamic consistency of the model, we have to respect the Clausius-Duhem inequality:

$$\boldsymbol{\sigma}: \dot{\boldsymbol{\varepsilon}} - \rho\dot{\psi} \geq 0 \qquad (8)$$

This inequality can be verified if we achieve to respect:

$$\frac{\partial\psi}{\partial d^t}\dot{d}^t \geq 0, \frac{\partial\psi}{\partial d^c}\dot{d}^c \geq 0 \tag{9}$$

Considering equation, one gets for the first term of each inequality:

$$\frac{\partial\psi}{\partial d^t} = \psi_0^t, \frac{\partial\psi}{\partial d^c} = \psi_0^c \tag{10}$$

By definition, ψ_0^t and ψ_0^c are always positive. As a consequence, we only have to ensure a positive evolution of the damage variables d^t and d^c to verify the Clausius-Duhem inequality. This condition can be simply imposing on the damage evolution law.

The damage thresholds are defined according to equivalent strain criteria. As the nonlinear behavior is decoupled in two parts in order to obtain unilateral effect, two equivalent strains are defined ε_{eq}^t and ε_{eq}^c:

$$\varepsilon_{eq}^t = \sqrt{\sum_{i=1}^3 \langle\varepsilon_i^t\rangle_+^2}, \varepsilon_{eq}^c = \sqrt{\sum_{i=1}^3 \langle\varepsilon_i^c\rangle_+^2} \tag{11}$$

with ε_i^t the eigenvalues of the strain tensor $\mathcal{H}[\mathrm{Tr}(\widetilde{\boldsymbol{\sigma}})]\boldsymbol{\varepsilon}$ and ε_i^c the eigenvalues of the strain tensor $\mathcal{H}\big[\mathrm{Tr}(-\widetilde{\boldsymbol{\sigma}})\big]\boldsymbol{\varepsilon}$. Loading surfaces are defined for both nonlinear domains:

$$f^t = Y^t - \varepsilon_0^t, f^c = Y^c - \varepsilon_0^c \tag{12}$$

With $Y^t = \max(\varepsilon_{eq}^t, \varepsilon_0^t)$ and $Y^c = \max(\varepsilon_{eq}^c, \varepsilon_0^c)$. The masonry under compressive loadings shows a hardening then softening behavior. To this aim the evolution law proposed initially proposed for concrete under compressive loadings is considered.

$$d^t = 1 - \frac{\varepsilon_0^t}{Y^t}\exp[-B^t(Y^t - \varepsilon_0^t)] \tag{13}$$

with B^t the model parameters which control the evolution shape of d^t and ε_0^t the equivalent strain threshold associated to the first cracks under tension.

$$d^c = 1 - (1 - A^c)\frac{\varepsilon_0^c}{Y^c} - A^c\exp[-B^c(Y^c - \varepsilon_0^c)] \tag{14}$$

with A^c and B^c the model parameters which control the evolution shape of d^c and ε_0^c the equivalent strain threshold associated to the first cracks under compression. In order to ensure mesh objectivity with the softening behavior, an Hillerborg method is used. The parameter B^t is adjusted in order to dissipate the same energy in an element whatever its characteristically size h:

$$B^t = \frac{f^t h}{G_f^t}$$

with G_f^t stands for the energy dissipation identified by uniaxial tension test and f^t for the peak stress in tension.

For the proposed application, a plane stress condition is considered (i.e. shell element formulation). In order to get this plane stress state, the out-of-plane component is imposed directly equal to zero.

3.2 Numerical calibration process

The parameters of the continuous model have been identified thanks to the virtual test data obtained with the discrete model: a compression test and a tensile one. The parameters to be adjusted are the Young modulus, the tensile strength, the compressive limit strain, the energy dissipation, and the coefficients B^c and A^c controlling the evolution of damage in compression.

The elastic parameters, Young modulus, Poisson's ratio and material density, have been taken identical to those of the experimental tests. The listed parameters have been identified thanks to an optimized calibration technique. An error function, which describes the distance gap between the discrete model curve f^{DEM} and the one of the continuous model f^{con}.

$$F_{error}(\boldsymbol{x}) = \sum_{i=0}^{n_{end}} \sqrt{\frac{\left|f_i^{DEM} - f_i^{con}(\boldsymbol{x})\right|}{\left|f_i^{DEM}\right|}} \tag{15}$$

It depends only on the five nonlinear parameters $\boldsymbol{x}$ of the damage model. Thanks to a minimization process using the GRENAT tool **Erreur ! Nous n'avons pas trouvé la source du renvoi.**, an identification of these parameters is made. It provides very inexpensive approximate responses of the objective function and enables to achieve a global optimization and to obtain the global minimum. The process only requires to test 2^5 parameter combinations, which represents only 2 hours for the tensile test with a simple 12Go memory and 64bits computer.

As a first verification of the model efficiency and the calibration process, Fig. 5 compares the behavior under monotonic compressive load of the discrete and continuous models with the experimental test results of **Erreur ! Nous n'avons pas trouvé la source du renvoi.**. Fig. 5 shows also that the continuous model tensile behavior perfectly matches the one of the discrete model. One can notice that the overall behavior is well reproduced and the limit strengths are correctly estimated in both cases.

For further validation we then have used the shear test under a constant 1 MPa axial compression stress previously used in section 2.3. The figure 7 validates of the simulated response with the continuous model by comparing it with the discrete results previously validated. The simulated response is quantitatively similar until a 1m displacement. Then it gradually diverges as for the discrete model compared to the experimental results.

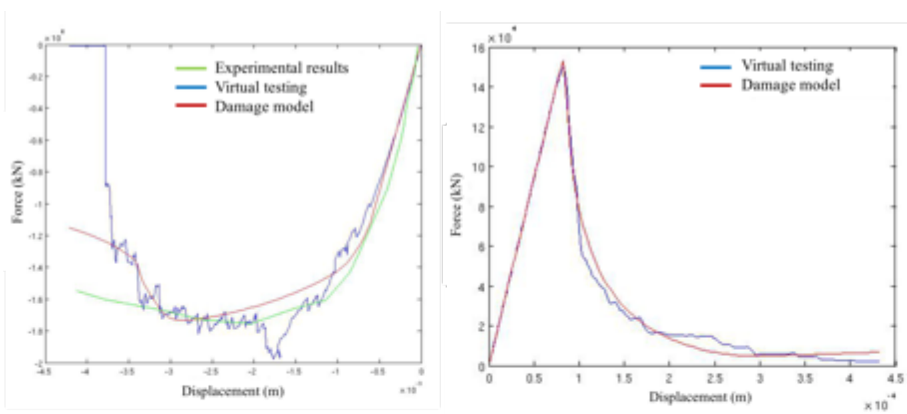

Fig. 5 – Response of the old masonry wall for various loading: compression (left) and shear (right).

The continuous calibrated model can then be used at the structural scale. It has to be pointed out, even if a simple continuous model is considered here, this procedure can be easily used to identify more complex model with a larger set of parameters. An application of this model to a complete old masonry structure is now presented. To take into account the specificities of each church and the characteristics of its materials, we modify its elastic parameters, according to in-situ modal data.

4. Analysis of an old masonry structure

4.1 Description of the church

The Notre-Dame de la Gorge church (NDG) is located in the Chamonix- Mont Blanc Valley in the French Alps, at 1250 meters above the sea level. The ground slope between the entrance facade and the choir is greater than 15%. NDG has been built between 1699 and 1701, and exposes some precious baroque cultural assets: statues, reredos, paintings **Erreur ! Nous n'avons pas trouvé la source du renvoi.**. As shown in Fig. 6, NDG has a single nave, with a rectangular tribune above the first span of the nave. The choir and the sacristy are 3.5 m narrower than the nave, and 3 steps above it. They are covered by a lower roof than the one over the nave, which is ended by an important cantilevered part over the entrance facade. The bell tower is placed along the nave, and covered by an onion shaped roof. During the Revolution it has been transformed into a stable, then very little maintained during the 19th century, which explains the structural evolutions such as modifications of the openings or the addition of a small lintel.

The masonry is very rustic, with an important proportion of mortar and small irregular stones. No data was available regarding its mechanical characteristics but the disposition of the stones and the materials are considered to be close to the ones in 0. As a consequence, the nonlinear parameters considered are the ones identified previously. The only paired stones are in the basement of the bell tower and in the corner of the entrance facade. As showed in Fig. 6, cracks are numerous, especially around the openings, between the nave and the choir, and in the vaults. Some of them are opened through the entire wall, such as in the entrance facade.

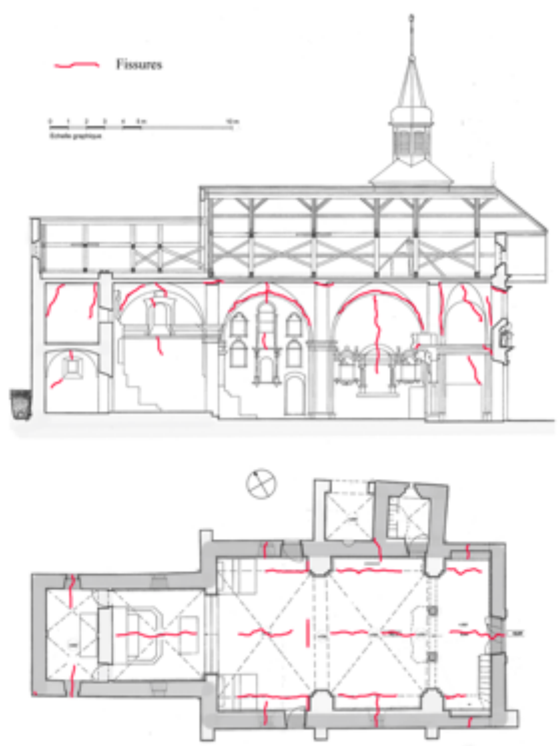

Fig. 6 – Plan and longitudinal section of NDG church. Cracks noticed during the field survey.

4.2 Finite element model

The mesh of the structure has been developed from plans and in-situ measurements (i.e. laser pointing and photogrammetry). The elastic parameters of the different parts of the church have been identified thanks to modal updating. The proposed method for the modeling of the whole building and the modal updating of the global model is explained in **Erreur ! Nous n'avons pas trouvé la source du renvoi.**. All computations have been performed with the finite element code Cast3M **Erreur ! Nous n'avons pas trouvé la source du renvoi.**.

Pilasters, buttresses, arches and structural elements of the framework such as the belfry, the onion shaped bulb and the inferior purlins in the choir and the nave, are modelled with beam elements. For the masonry elements multifiber beam elements with nonlinear material laws are considered.

Walls, vaults and tribune are described with multilayer shell elements. Even if it is a strong assumption, **Erreur ! Nous n'avons pas trouvé la source du renvoi.** has shown with parametric tests that shell elements allow obtaining relevant results for an entire structure under seismic loading. The masonry of each substructure of NDG is characterized by a tensile strength $f^t = E.\varepsilon_0^t$ depending of its Young modulus, which has been identified during the modal updating.

The Vallorcine earthquake (2005) is considered as a loading, which is representative of the seismic activity in the studied area (Fig. 7). This strongest earthquake recorded in the area since the establishment of the instrumentation is well below the reference accelerations.

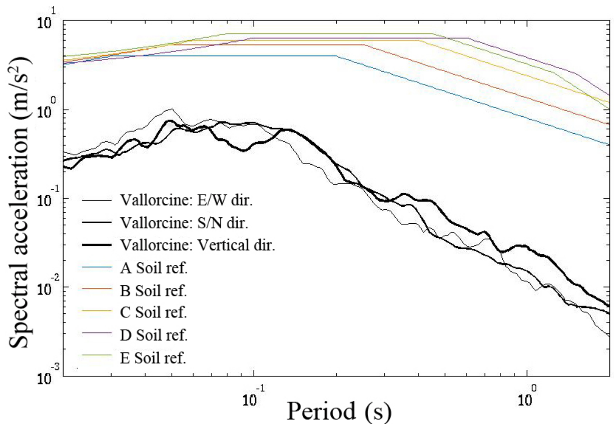

Fig. 7 – Spectral acceleration of the Vallorcine earthquake and the regulatory earthquakes.

Fig. 8 shows the tensile damage field (d^t) at the end of the 22 seconds signal. One can notice the concentration of the damage in the vaults. The computed damage areas are consistent qualitatively with the history of the disorders observed in the studied churches, as shown by the comparison with Fig. 9.

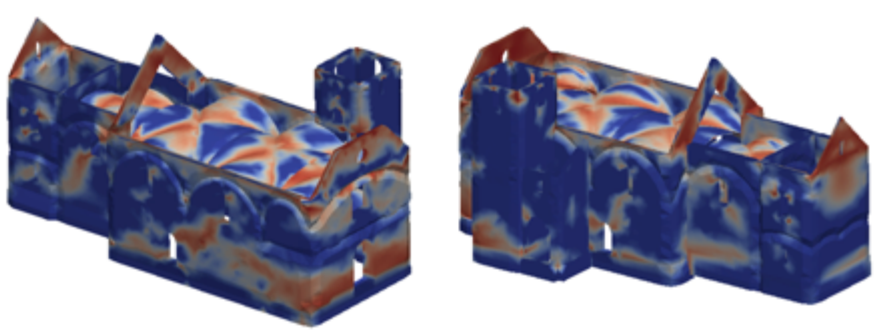

Fig. 8 – Damage field at the end of the Vallorcine earthquake (2005).

Fig. 9 Surveyed damages in NDG.

Conclusion

In this work a global methodology for the seismic vulnerability assessment of an entire non-paired masonry structure from the material behavior up to the structural response has been proposed. At the material scale, a virtual testing tool, initially developed for concrete, has been adapted for non-paired old masonry. A comparison with experimental data from the literature has shown the capacity of this tool to efficiently reproduce the nonlinear behavior of the masonry.

At the structural scale, it stays necessary to have a material model which allows taking into account the highly nonlinear behavior of masonry under seismic loading while keeping a relatively small computational time. To fulfil this requirement, an isotropic continuous damage model has been considered. In order to identify the parameters of this model and to investigate different loading paths, the virtual testing tool has been used. This identification process is a very interesting answer to many problems encountered in CuHeS assessment, particularly the difficulty to manage in situ tests and to replicate the real loadings in laboratory tests. In order to illustrate the whole process, the response of a church under seismic loading has been studied. The main damages observed on the structure have been retrieved considering a historical earthquake in the region of interest.

As perspectives, the development of a full 3D version of the virtual testing tool could allow to describe out-of-plane crack and additional ruin mechanisms of the masonry wall. Furthermore, the influence of the out-of-plane heterogeneity of the wall could be investigated. Concerning the macroscopic model, more complex models can be identified. Indeed, the capacities of the virtual testing tool have not been fully used as the description of friction during cyclic loading. It has been shown for applications on concrete that hysteretic phenomena can be efficiently identified with this virtual testing tool.

References

B., Silva. 2012. *Diagnosis and strengthening of historical masonry structures: numerical and experimental analyses.* Ph. D. thesis, Padova: University of Padova.

Binda L., Fontana A., Frigerio G. 1988. "Mechanical behaviour of bric masonries derived from unit and mortar characteristics." *8th International Brick and Block Masonry conference.* London: Elsevier Applied Science. 205-216.

CEA. 2016. "Finite Element tool box for Structural and Fluid Mechanics." April. http://www-cast3m.cea.fr/html/presentation/Plaquette_Cast3M_2015_numerique_en.pdf.

Faria R., Oliver J., Cervera M. 1998. "A strain-based plastic viscous-damage model for massive concrete structures." *International Journal of Solids and Structures* 35 (14): 1533-1558.

J.V., Lemos. 2007. "Modeling of historical masonry with discrete elements ." *International Journal of Architectural Heritage: Conservation, Analysis, and Restoration* 1 (2): 190-213.

Laurent L., Boucard P.-A., Soulier B. 2013. "A dedicated multiparametric strategy for the fast construction of a cokriging metamodel ." *Computers and Structures* 124: 61-73.

Limoge-Schraen C., Giry C., Desprez C., Ragueneau F. 2015. "Toward a large-scale seismic assessment method for heritage building: Vulnerability of masonry baroque churches." *European Journal of Environement and Civil Engineering* 20 (6): 680-710.

P., Casarin. 2006. *Structural assessment and seismic vulnerability analysis of a complex historical building.* PhD thesis, Trento: University of Trento.

Silva B., Guedes J. M., Arêde A., Costa A. 2012. "Calibration and application of a continuum damage model on the simulation of stone masonry structures: Gondar church as a case study." *Bulletin of Earthquake Engineering* 10 (1): 211-234.

Vassaux M., Oliver-Leblond C., Richard B., Ragueneau F. 2016. "Beam-particle approach to model cracking and energy dissipation in concrete: Identification strategy and validation ." *Cement and Concrete Compositions* 70: 1-14.

Vassaux M., Richard B., Ragueneau F., Millard A., Delaplace A. 2015. "Lattice models applied to cyclic behavior description of quasi-brittle materials: advantages of implicit integration." *International Journal for Numerical and Analytical Methods in Geomechanics* 39 (7): 775-798.